Available online at www.jrors.ir

Journal Of Radar and Optical Remote Sensing

JRORS 1 (2019) 58–70

Rockfall Detection Using Differential Interference Synthetic Radar Technique from Sentinel-1 Satellite Imagery (Case study: Haraz road)

Omid karimi[a], Seyyed Ali Almodaresi[b *]

[a]*MS in GIS, Remote Sensing, Yazd Branch, Islamic Azad University, Yazd, Iran*
[b]*Associate professor, GIS and RS Department, Yazd Branch, Islamic Azad University, Yazd, Iran*

Received 16 December 2018; revised 20 May 2019; accepted 26 May 2019

Abstract

Massive material movements are natural geomorphic processes. This process refers to separation and downward transportation of soil and rock materials under the influence of gravity and causes the transfer of a large amount of material, such as pebbles. In Iran, the given climate, geology and topography, massive movements, debris, conditions results in low altitude areas, significant casualties, financial and environmental damages. Modeling physical processes of rockfall calls for examining the fracture of rocky elements, dimensional fall or jump, crushing, rotation, or slipping and the final subsidence, regardless of the volume constraints of rockfall which are defined by their high energy and mobility. Dynamic processes of rockfalls are overshadowed by spatial and temporal distribution properties, including the disruption conditions, geometric and mechanical properties of the rock blocks and rocky slopes. One of the most suitable methods for identification of rockfall phenomenon is using radar interferometry (D-INSAR) technique. The study examined Haraz road with twelve Sentinel 1 sensor images from March to May 2016. Then, using an interferometry technique of radar with artificial aperture, the rockfall rate of SAR data related to Sentinel 1 sensor was measured, obtained in high and low pass modes. In addition, three rockfalls registered on March 20, 2015, March 31, 2015, and May 10, 2015 were examined in this study. The results showed that the rockfall times in all three pilot maps of displacement have significant changes compared to the unchanged times in the images. Using radar satellites and differential interferometry techniques, one can detect the amount of rockfall and its location.

Keywords: INSAR, Rockfall, Hezar Road, Sentinel 1, Ascending, Descending

* Corresponding author. Tel: +98-9131526455.
E-mail address: almodaresi@iauyazd.ac.ir.

1. Introduction

The incidence of natural disasters causes significant damage to life, financial and environmental impacts throughout the world every year. Massive motions are specific forms of nature and incidents of range processes caused by geomorphologic, hydrologic and local geological conditions. These conditions along geodynamic processes, vegetation, land use, amount, intensity, and continuity of rainfall and earthquakes can end in the formation of rockfall (Madaldost, 2008).

Rockfall involves the sudden or rapid movement of loosen blocks or a set of hard stones separated from sloping rocky walls that usually occurs along the layers of the joints and fault zones or fault surfaces (Chayo, Tang and Wang, 2004). Rockfall is one of the most common forms of slopes in mountainous areas with its distinction from other instabilities being high and sudden incidence. Thus, rockfall is among the most devastating massive movements ending in loss of life and heavy damages.

In most cases, the hazards of rockfall cannot be nullified as the occurrence of such dangers are diverse spatially and temporally. Basic statistics methods, are mostly done with the help of computer modeling, has become a standard tool for evaluating the risk of rockfall and designing protective measures. The modeling of the physical processes of rockfall needs examination of the fracture of the rocky elements, falling or jumping, and dimensional jump, crushing, rotation, or slipping and final subsidence Hutchinson (1998), Evans and Hanger 1993, and Gazeti et al. (2002). Regardless of the volumetric constraints, rockfalls are characterized by their high energy and mobility. Dynamic processes of rockfalls are overshadowed by spatial and temporal distributions, like fracture conditions, geometric and mechanical features of rocky blocks and rocky slopes (Jaboudov et al., 2005).

The rockfall causes damages, blocks roads and razes the villages and fields to the ground. Among 368 rockfalls in Hong Kong from 1984 to 1996, 35% have caused obstruction or damage to roads, 22% damage or evacuation of buildings, 21% roadside obstruction and 6% damage to the car and public services. Only 15% of these incident occurred on the open ground, leading to negligible effects on human activities. The studies on rockfalls and evaluation of their danger in various areas can be found in the studies of Batterson et al. (2006), and Binal and Ercanoglu (2010). In Iran, in his master thesis, Gholami (2004) located rockfall risk using geographic information and remote sensing along Haraz Road from Vana to Plor. The study considered four factors of petorolgy, gradient, elevation relative to the road surface, and distance between driver's view to make decisions and react to falling rocks. Ghazipour et al. (2006) used the theory of cone of depression in evaluating the risk of rockfall. In the study of Chalus road (Zangouleh Bridge to Marzanabad), it was shown that the risk of rockfall has a direct relationship with the slope of the rocky slopes and its topographic conditions. Moreover, the type of the rock has an important role in the expansion and formation of rockfall.

In Iran, studies on the zoning of slopes are recent and their serious start dates back to the early 90s and 2000. Here are some of the studies in Iran. Gholizadeh (2010) examined the rockfall potential in Zangbar of Macau using 18 parameters and field observations and using the fuzzy model. Golizadeh concluded that gamma operator 0.7 is the most suitable operator in determining the capability of falling in the studied basin. Using cluster analysis method, Esfandiari Dorabadi and Hashemi (2012) tried to map the risk of fall in Paveh communication pathway, stating that human factors such as land use change, vegetation decline, change in slope geometry, and communication paths on the slopes cause fall in the region.

Lan, Martin, Julio and Leim (2010) used a three-dimensional LIDAR data model to evaluate the risk of fall along the Canadian Iron Canal and used microscopic records to calibrate physical processes. They introduced a high-resolution digital model based on LIDAR data comprehensively. Dauart and Marquauens (2002) studied the spatial distribution of regional scale loss using topographic data in the GIS, and concluded that the combination of falls with geological map and digital land model led to a strong correlation between the fall and petrology, altitudes, altitudes, slopes, rock walls and waterways. Regarding this, it is necessary to provide suitable measures for environmental and regional planning in the study area by identifying the risk of collapse hazard assessment with radar interferometry, while providing solutions to reduce damage.

Radial differential interferometry is an effective method for measuring the displacement of ground surface. Thus, using this technology, it is possible to closely monitor the movements of the ground surface continuously, with high precision and in a wide range. Given the extensive coverage of satellite images, synchrony and being low cost compared to other field methods, the use of this technology is very common

in the study of natural hazards of the ground like landslides, subsidence, quakes and volcanic activity. Radar interferometry capability in landing detection and tracking have already been reported by Gabriel et al. (1989) and Massonnet and Feigl (1998). Indeed, recent progresses in radar surveillance such as differential interferometry (DInSAR) have attracted the attention of many researchers and experts involved with landslide monitoring and assessment of environmental hazards, and the ability of this technique to detect and monitor landslide motions in various studies has been reported by Rott et al. (1999) Strozzi et al. (2005). In this paper Rockfall detection using differential interference synthetic radar technique from Sentinel-1 satellite imagery is investigated.

2. Materials and Methods

2.1. The Study Area

Road 77 or Haraz Road, along Road 59 (Karaj-Chalous), is the main road of Tehran-Mazandaran. This road passes through the valley of the Haraz River and is the closest main road to Damavand summit. This road describes the history of the enormous Alborz, Damavand, Amol and Iran. Moreover, the road is the shortest route between Tehran and Amol. It is estimated that only in Nowruz festival, the road hosts 5 million passengers. The Haraz road has 14 tunnels, with the longest one being over 1500 meters long. The construction of this road took 23 years (Figure 1).

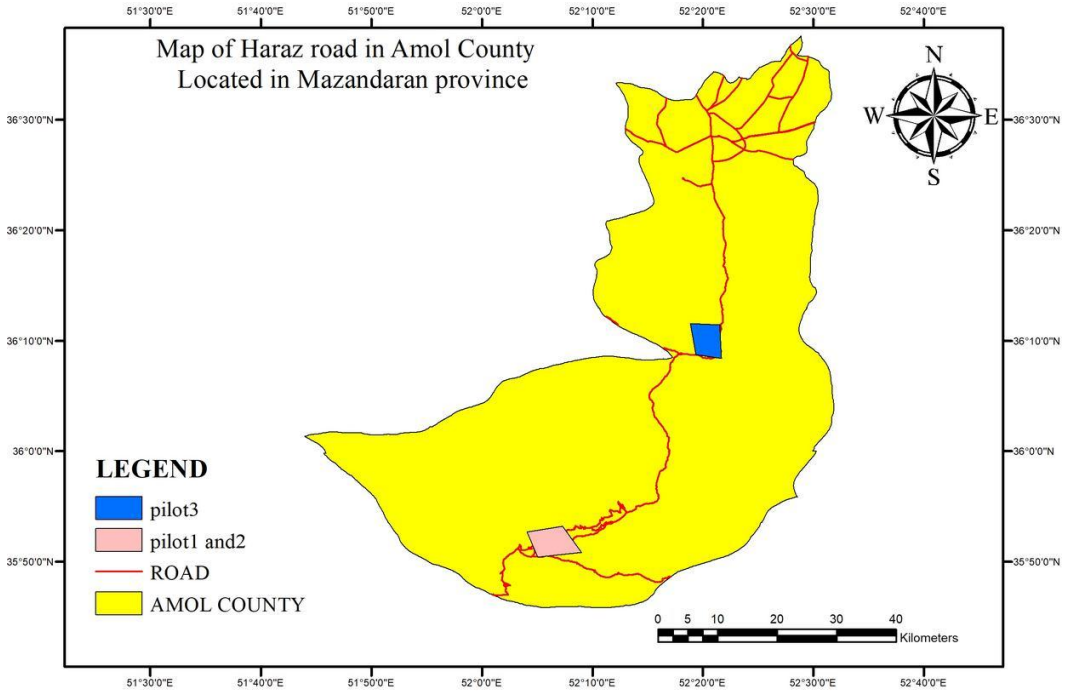

Figure 1. The studied area

2.2. Data

The data used in this study falls into general data of land and satellite data. The satellite data is collected from the European Space Agency and land data from the Office of Regional Water Studies of Mazandaran and the National Mapping Organization. Later on, the preprocessing and preparation operations on each of them will be mentioned.

2.2.1. Radar Sensor Data

The Sentinel 1 satellite was launched on April 3, 2014 by the European Space Agency. This solar satellite tracks a near-polar orbit at an altitude of 693 km. About 175 minutes is needed for the satellite to

spin around the earth for a full round and it takes 12 days to re-capture from anywhere on the planet. In this study, Sentinel 1 satellite imagery was used in the period from June 2016 to November 2016 from the Sarayan area.

Sentinel 1 SA1 Sensor

SA1 is a microwave sensor that captures C-wavelength in different modes. This sensor can, by interpolating the precision of less than one millimeter, show the displacement of the surface of the earth.

Table 1 shows the Sentinel 1 SA1 images used in this study, along time intervals and spatial basis lines.

Table 1. Sentinel 1 SA1 images used in the series with details

Table	Image state	Image mode
13/03/2015	Descending	IW_SSV
30/04/2015	Descending	IW_SSV
24/05/2015	Descending	IW_SSV
24/03/2015	Ascending	IW_SSV
17/04/2015	Ascending	IW_SSV
11/05/2015	Ascending	IW_SSV
24/04/2015	Ascending	IW_SSV
18/05/2015	Ascending	IW_SSV
11/06/2015	Ascending	IW_SSV
30/04/2015	Descending	IW_SSV
24/05/2015	Descending	IW_SSV
17/06/2015	Descending	IW_SSV

2.2.2. Rockfall Data

Based on the data for 2015 in April, May and March 2014, there have been rockfalls on Haraz Road in three different areas, used for this study.

2.3. Methods

2.3.1. Differential Radar Interferogram Technique

This is a method for combining SAR images from radar sensors mounted on a satellite or aircraft to create elevation maps, displacement and ground changes, or determine target speed. INSAR is capable of detecting displacements with a precision of millimeters, whereas DEM obtained from the laser is an accuracy altimeter 10 centimeters. In order to determine the switching of the Altimeter laser, the second DEM of the region should be reduced from the first DEM. Thus, the precision of determining displacement is 10 centimeters, which is less accurate than InSAR. Thus, the Altimeter Laser can provide more accurate DEMs and less precise mapping than InSAR. However, it is important to note that the Laser Altimeters takes up a small amount of bandwidth, and it has to overlap a large number of impressions to form a DEM comparable to DEM derived from InSAR.

2.3.2. DInSAR Method

DinSAR's differential reference vector expresses an estimate of surface changes (both in terms of surface and altitudes) by interferometry. The base for this is similar to the terrain mapping for data collection in the preparation of a map of the lattice size that was prepared 5 years ago and a map of the

raster map prepared a week ago (Raster map made of pixels whose numerical values of pixels represent the altitudes). If the two maps are exactly the same, two images of an array of zero will be obtained from pixel-to-pixel difference. If some values in the resulting image (non-zero image difference) indicate that there has been a change, the amount of change is proportional to the brightness value of the pixel in the resulting image (differential). Indeed, here we have used the map of the first (old) roster curve to remove topographic effects from the newer map. Likewise, it can be used for two DEMs from SAR images prepared before and after an important event such as a quake. The difference between the two interferometer causes the variation in the level of the quake. To produce two DEMs, four SAR images are needed in SLC format. As the first DEM derived from the interferometer should show a good approximation of the height of the earth, then it should be by a pair the radar image is produced with long open lengths. Thus, the second DEM derived from the iterphrometry should have the highest level of detail. A shorter open-coupled image should be obtained. In case of Target (such as the iceberg), the open length for the second pair of SAR images in the SLC format must be shorter. The length of the open line should be 300 m, 20 m and 5 m to generate DEM to study the motion of the earth and the applications of motion analysis (Paul, 2011).

2.3.3. Interferometer Processing

To provide interferogram with proper coupling of SLC images, relatively high coherence, accurate orbital parameters and appropriate open-ended line lengths can be processed. In a process aimed at producing a DEM, it should be used over longer spatial and shorter intervals, but in operations like this one, the purpose of which is to produce a displacement map, it should be selected at a given time interval (can be a year) data that has a low open length so that higher levels of symmetry between phases can be evaluated at 1 t and 2 t.

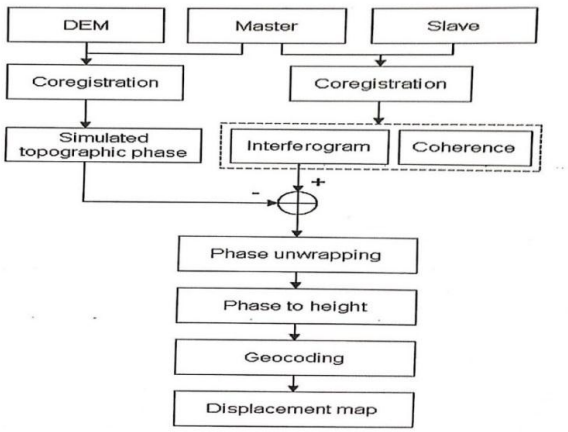

Figure 2. Processing stages in the production of interferogram and the displacement map in the DInSAR method

Mathematically speaking, an interferogram is produced by multiplying an SLC image in the complement antimatter of other SLC image. Remember that in SLC images, the open-distribution features of 1 pixel are represented by a 32-bit mixed pair.

Regarding this, the interferogram provides ground displacements in the interval between two shooting times in form of a displacement image not calibrated to a specific surface level or a definite image system. This is because the interferogram is expressed in the direction of the suffering of the mile; this is due to the fact that most SAR systems are patchy. Thus, first, the interferogram should be converted to horizontal (meaning vertical vision from above). The next step involves the wrapping of the interfrometransfer map. According to the above mentioned elements of the interferometric interactions and the relationships discussed in previous sections, interferogram was generated using sentinel1 sensor images using SARScape software for each of the studied regions.

3. Results

This part explains the details of the methods used to reach the research objectives. Using the data and method described in detail in the materials and methods, the results and outputs from the processing of Sentinel 1 images were examined. Initially, interferometry differential radar technique was used to calculate interferogram, and then using the interferogram of the map, two-axis was calculated and the maps were moved in each step. The research steps are described in Figure 2. Interfere-meters were performed in each of the upper and lower passes of the images for individual interferometry, and were discussed in different regions, the interferogram logs are shown below. The details of the produced interferogram are shown in Table 2:

Table 2. Baseline details

Pilot number	Image type	Image mode	Date	Temporal Base line(day)	Spatial Base line (meter)
Pilot 1 and 2	Ascending	IW_SSV	13/03/2015	48	145.11
		IW_SSV	30/04/2015		
		IW_SSV	30/04/2015	24	89.35
		IW_SSV	24/05/2015		
	Descending	IW_SSV	24/03/2015	24	12.60
		IW_SSV	17/04/2015		
		IW_SSV	17/04/2015	24	43.5
		IW_SSV	05/11/2015		
Pilot 3	Ascending	IW_SSV	24/04/2015	24	74.25
		IW_SSV	18/05/2015		
		IW_SSV	18/05/2015	24	73.63
		IW_SSV	11/06/2015		
	Descending	IW_SSV	30/04/2015	24	84.25
		IW_SSV	24/05/2015		
		IW_SSV	24/05/2015	24	76.32
		IW_SSV	17/06/2015		

3.1. Interferogram Production

The interferometer contains the phase difference between two images. The altitude is determined at each point of the region at the time interval between the two images by the phase difference check. The interlacing is made by the mixed blend of the original image in conjunction with the dependent image.

Removal of the effect of photographed topography due to interferometry using the digital earth model (DEM), the effect of the topographic phase can be eliminated from the interferometer, the more accurate

the DEM and the orbital information of DORIS, the better the removal process is done. The results of this step are to remove power from phase and generate power file, dpf, int, sint, dint, and shp srdem power.tif. It should be noted that the difference between int and dint is that there is topography in the int file, but there is no topography in the dint. There may be three attributes in the int file called Ramp, Jump, Bamp. The phase changes and looks like a dome. If Bamp is available, the fringe is formed in the form of concentric circles with the same diameter.

3.2. Applying Filter

The resulting differential interferometer contains some noises. The element producing these noises can be different, with two main factors affecting their creation. The first factor is the time difference between the two main and dependent images. Sometimes, changes in the area that occur between the time intervals of the two images are all about the noise that can be attributed to the construction of residential areas or agricultural activities in the region. The second major factor is the effect of the creation of noise. The point of reference is that the noise level in the images is directly related to the spatial basis, the higher the number, the more noise encounter in the interferometer.

Filtering has been used to remove and reduce noise. Due to the high efficiency of Goldstein's filter, it was used in the study. The result of applying the Goldstein filter is the production of interferometric filter, with more margins in comparison with non-filtered interferometric filter with significantly reduced noise level. The special feature of this filter is acting selectively, and the filtering operation is performed locally, the type of performance of the Goldstein filter is affected by the interferogram correlation, in some cases the degree of correlation is low, the amount of pixels is more affected. And in cases where the correlation is high, it affects the limited number of pixels which is made simultaneously with the filtering of the image of symmetry.

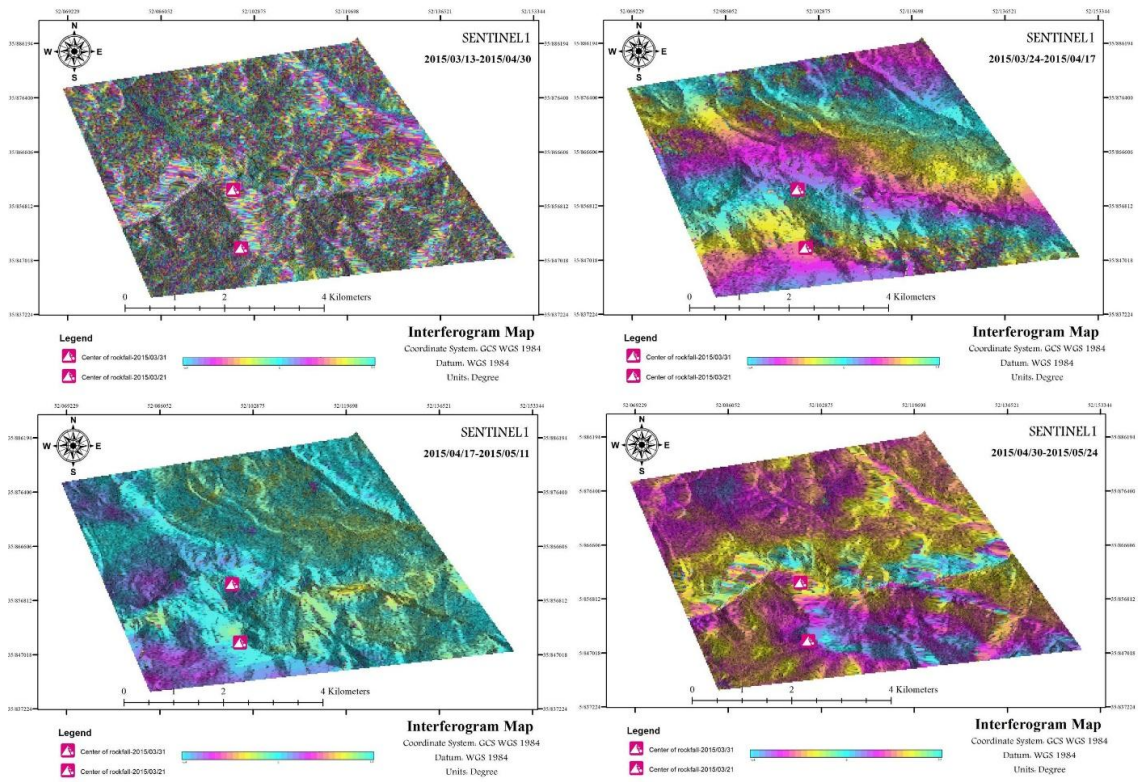

Figure 3. Interferogram Map

In the days March 20, 2015 and April 3, 2015, two elevations occurred at a distance of 2 km in the area

of Haraz road, as shown in Figures 3 and 4, of the interferometer for the low pass state and in Figures 5 and 6, it is related to the high-pass state.

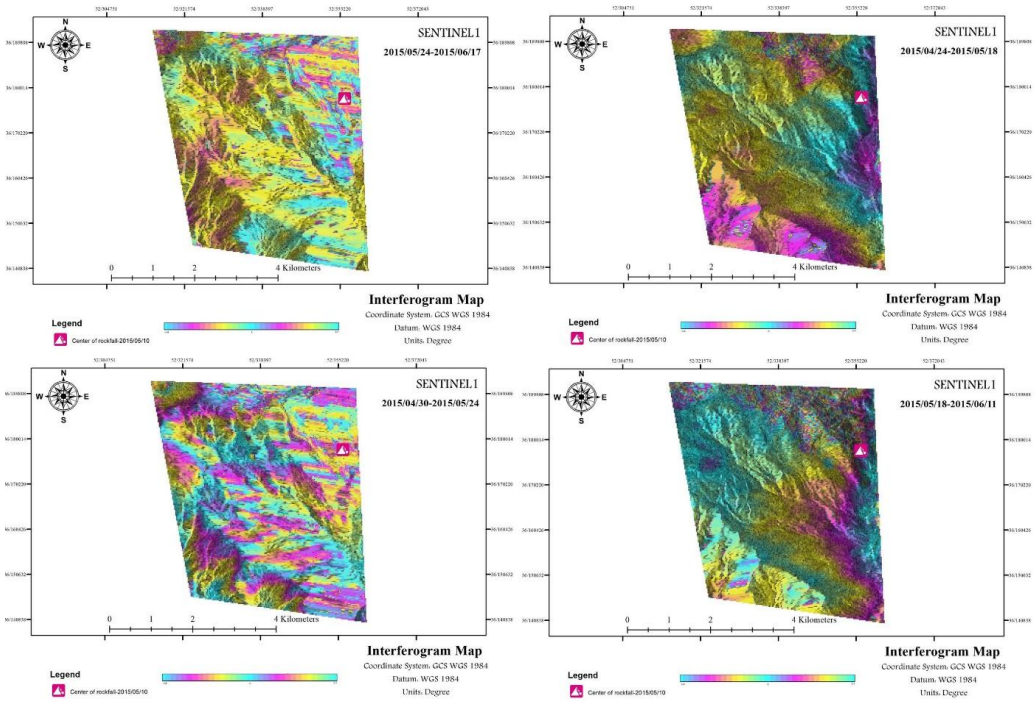

Figure 4. Interferogram map

One of the outputs of the interferometry radar technique is the coherence of the images used in the interferometer, as seen in Figures 5 and 6. The symmetry image is affected by the correlation between the coupled powers of the image. It has to be noted that the coherency image expresses the correlation between the original and dependent image signals. The degree of coherence is between 0 and 1, the pair of images whose zero-degree symmetry is zero, there is no signal-dependent relationship between them, and when the degree of symmetry is one, the signal dependency between the two images is 100%. The higher the degree of symmetry between the coupled images, the better the couple of images for the differential interferometry are, and an increase in the quality of the interlaced is witnessed.

$$\gamma = \frac{|\sum S_1(x).S_2(x)|}{\sqrt{\sum |S_1(x)|^2 . \sum |S_2(x)|^2}} \quad (1)$$

S_1 is the mixed value of the original SAR image, and S_2 is the mixed quantity of the SAR image, and γ is the degree of coherence between the two images. The degree of coherence expresses the accuracy of the results obtained, so that in images whose magnitude of coherence is close to 5.0 or higher, they are suitable images for interlacing, but in cases with values less than this, one can use them to construct interlacing (Anderson et al., 2008).

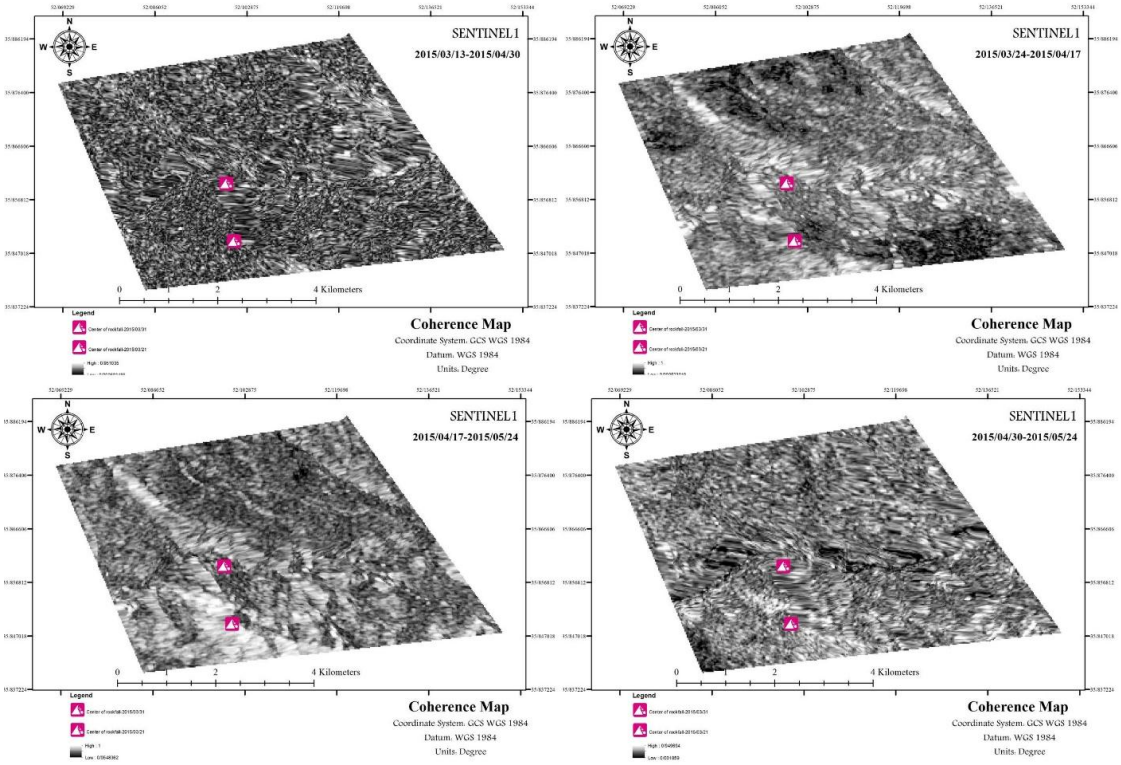

Figure 5. Coherence map

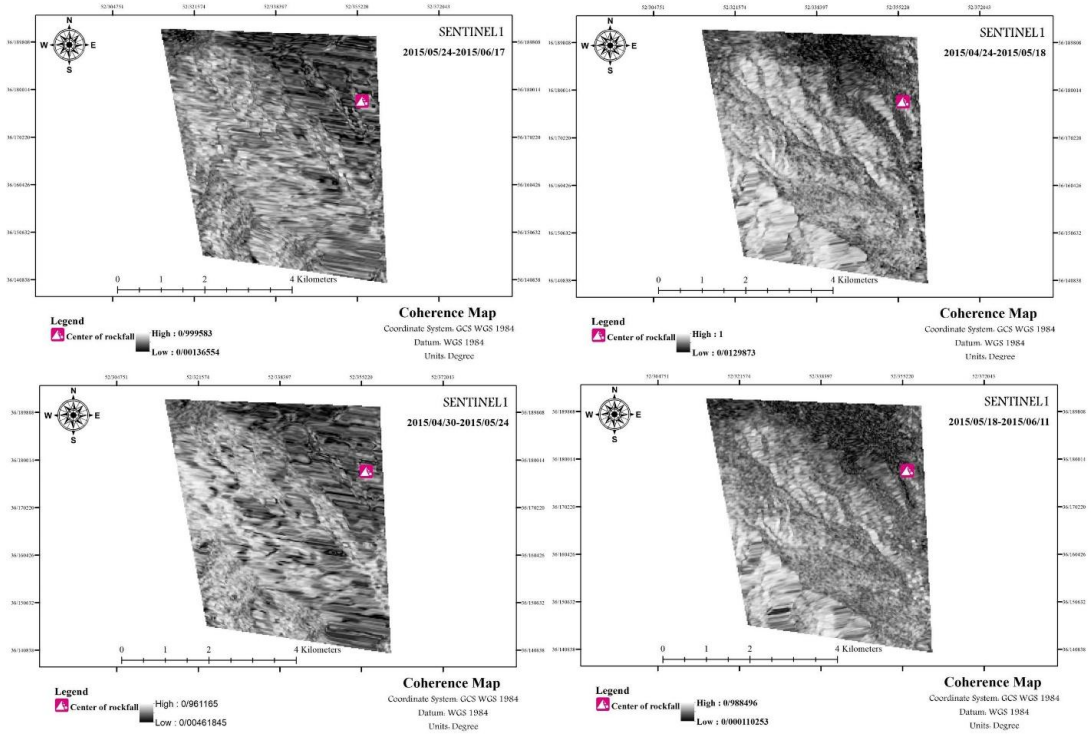

Figure 6. Coherence map

3.3. Sentinel 1 Sensor Displacement Values

After interferometry method on Sentinel 1 images and creating interlacing and after final processing in SARSCAPE software, they were converted to vertical displacement values in meters.

3.4. Absolute Phase Transformation to Displacement

The changes in the phase show the variations in height are half as wavelength, as the rockfall wavelength of the Sentinel 1 sensor is 5.6 centimeters. Changes of π2 equal lead to height change of 8.2 cm. With the removal of the orbital phase and the phase of the vibration of the platform, the absolute phase of the result can easily be converted to altitudinal displacements. In phase-to-altitude conversion, for each pixel, the value is equal to the magnitude of the elevation of that point in terms of metric. In subsidence maps, the negative values show the downward movement (subsidence). The entire process is used to the coupled images of Sentinel1 and results in the creation of descending maps at the time of taking pictures.

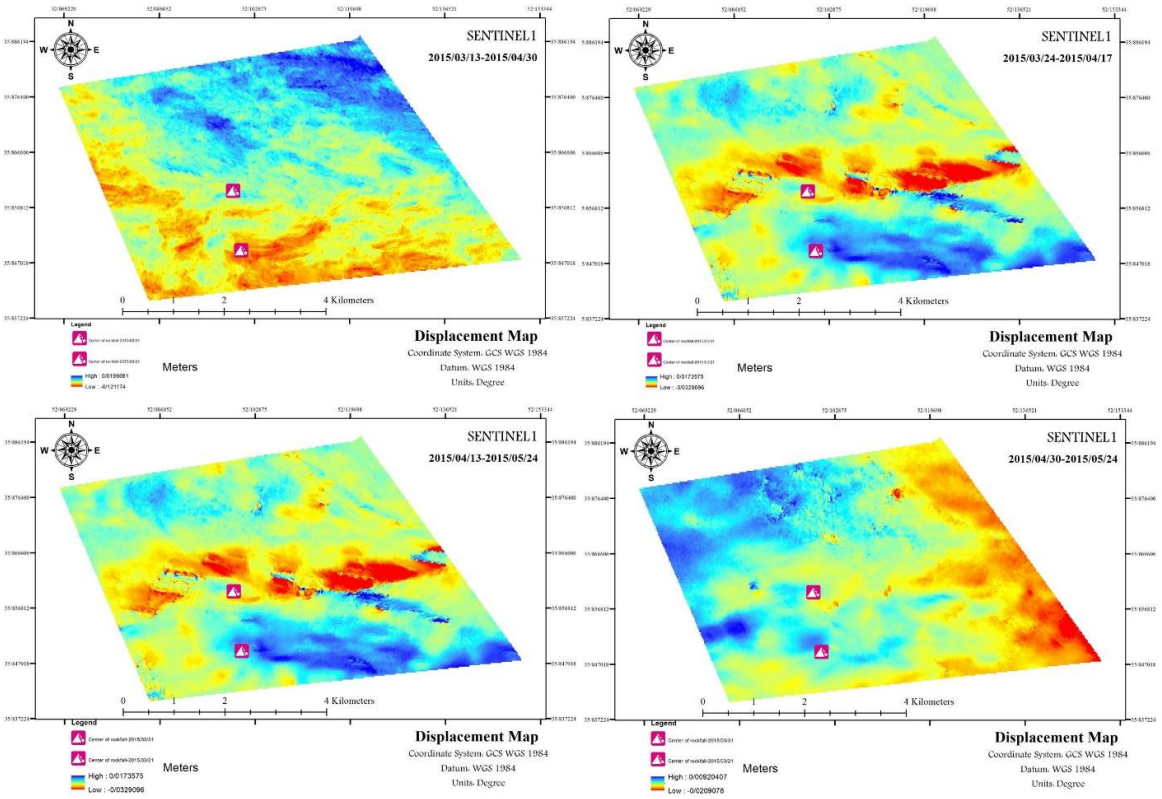

Figure 7. Vertical map of the Earth's surface

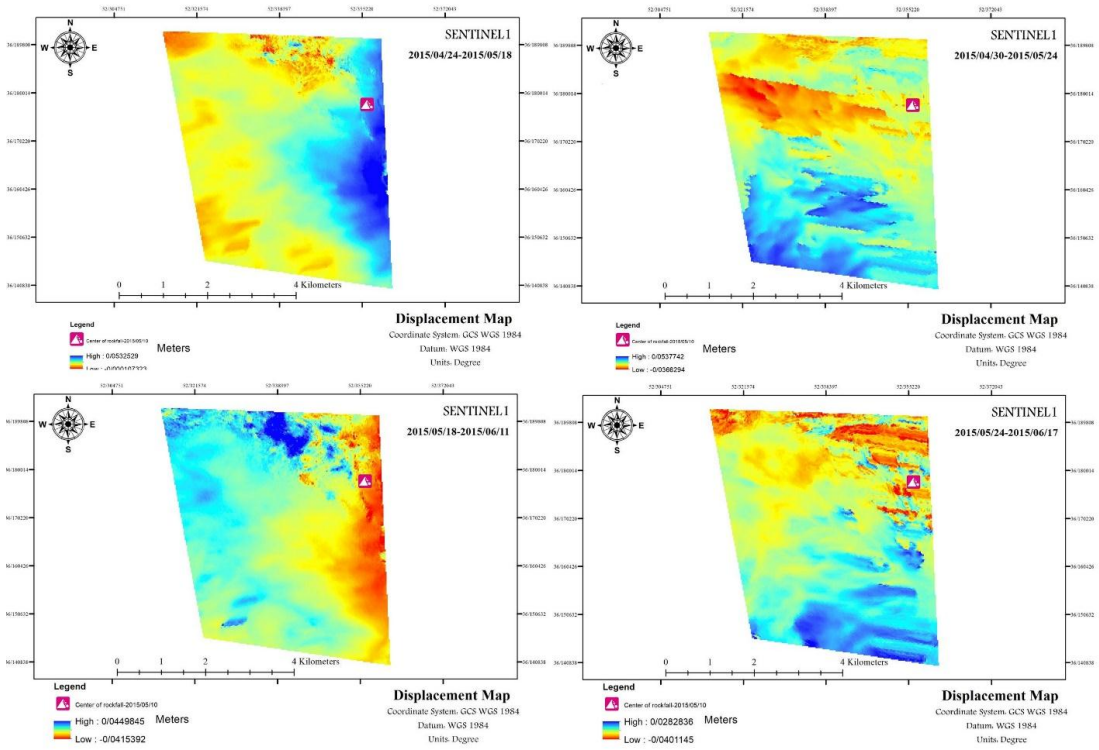

Figure 8. Vertical map of ground level

4. Discussion and Conclusion

Although rockfalls are physically affected by the slopes, they are subject to uncertainty and probability issues that must be calculated. A definitive polar modeling has problems with describing and evaluating complex natural processes, such as rockfall. Using interferometric radar method in this study, due to the adverse effects of massive movements and rock falls on the socioeconomic and natural systems, the need to understand areas sensitive to rockfall to avoid the risk and prevent the occurrence of financial losses, environmental, the initiation of protective and preventive measures (Krum, 2001). The fall of the rocks is the result of the separation of large and small parts of the rocky slopes. The small and large pieces of massive rock phenomena simultaneously fall into large masses, called “fall” (Mahmoudi, 2011), as other phenomena of geomorphology, the result of several factors and also the result of the interaction of different factors on each other. The material of the bed of the massive movements, the slope of the valley domain, the land use, the fault, the lines of communication and drainage, and so on are among the factors influencing the occurrence of these phenomena. Tomas, Vinowich and Anderson (1995) stated that massive motions in rock slopes, sandstone formations and limestone were introduced with more rockfalls. Compared to the landslide phenomenon, few studies have been constructed in Iran regarding fall. In the study, Gholami (2004) examined the risk of rockfall using GIS and remote sensing along Haraz road from Vana to Plor. In this study, four factors of lithology, slope, elevation, and road distance were considered for decision makers and reaction to falling rocks. Bayati Khatibi (2007) has examined the zoning of high-risk and mountain slopes of the communicative network of villages located in Garnukuchai basin, where 10 factors were considered for zoning official susceptible areas. After weighing all the factors, the sensitivity of different parts of the area with five classes of sensitivity were obtained. Shirzadi, Mousavi and Kavian (2010) conducted a study entitled “The GIS of the Regional Model of Rockfall through Mountain Roads” with the help of the overlap index in Salavat turn in Abad of Kurdistan, using the rockfall density and allocating expert weights to the factors, showed a map of the risk of rockfalls in the study area. In this study, the accuracy of the zoning map for hazard locating of rockfall was "70%". Madal

Dost and Ooladzadeh (2010) used their research in 3D modeling the area of Imamzadeh Ali Jadat Haraz GIS as base for determining the path of rockfall in the environment. In this study, the descriptive statistics of the spill points, including the difference in length (m), the minimum length of the path, the maximum length of the path, the average length of the path and the distance to the point were determined and the distribution of the risk of rockfalls, rock placement and rock hazard zonation were achieved. Based on the discussions, it is shown that the use of radar interferometry with the help of INSAR algorithm in this study has a good capacity for determining the rate of land surface movement in the short and long terms. The wavelength C was introduced at the range of the study. Processed interferograms only have a short time line to reduce the lack of time correlation and their spatial bases are taller than the usual one, since the goal of the processing is a large number of interferograms in such a way that the intergroup chips are not discrete, but interferograms with the length of the base line. The high point is under the influence of topographic error. In the study, three different pilots of rockfall in two high and low passes were prepared before and after the rockfall of the interferometer. The findings showed that during interferogram extractive rockfall, spectacles have significant changes in the central part of rockfall. Moreover, the coherence maps created during these times have been modified in the direction of fall move. The above cases leading to the displacement maps at the time of the rockfall showed significant changes explained in details in the images. There was no accurate ground information on the volume of rockfall that the case made it impossible to compare satellite and ground data. Rockfalls are a major hazard in rock cuts for highways and railways in mountainous terrain. While rockfalls do not pose the same level of economic risk as large scale failures which can and do close major transportation routes for days at a time, the number of people killed by rockfalls tends to be of the same order as people killed by all other forms of rock slope instability.

Reference

Afzali, A., Sharifi Kia, M., & Shayan S. (2013). Assessing the vulnerability of infrastructure and settlements to the phenomenon of subsidence in the plain of Damghan. *Two letters of application form of geomorphology*, (1), 70-85.

Amighpey, M., Arabi, S., Talebi, A., & Djamour, (2006). Elevation changes of the precise leveling tracks in the Iran leveling network, Scientific report published in National Cartographic Center (NCC) of Tehran, Iran.

Motagh, M., Walter, T. R., Sharifi, M. A., Fielding, E., Schenk, A., Anderssohn, J., & Zschau, J. (2008). Land subsidence in Iran caused by widespread water reservoir overexploitation. *Geophysical Research Letters, 35*(16).

Chatterjee, R. S., Fruneau, B., Rudant, J. P., Roy, P. S., Frison, P. L., Lakhera, R. C., ... & Saha, R. (2006). Subsidence of Kolkata (Calcutta) City, India during the 1990s as observed from space by Differential Synthetic Aperture Radar Interferometry (D-InSAR) technique. *Remote Sensing of Environment, 102*(1-2), 176–185.

Raucoules, D., Colesanti, C., & Carnec, C. (2007). Use of SAR interferometry for detecting and assessing ground subsidence. *Comptes Rendus Geoscience, 339*(5), 289-302.

Esmaili, M., & Motagh, M. (2009). Remote sensing measurements of land subsidence in Kerman Valley, Iran, 2003-2009. In *AGU Fall Meeting Abstracts*.

Galloway, D. L., Hudnut, K. W., Ingebritsen, S. E., Phillips, S. P., Peltzer, G., Rogez, F. & Rosen, P. A. (1998). Detection of aquifer system compaction and land subsidence using interferometric synthetic aperture radar, Antelope Valley, Mojave Desert, California. *Water Resources Research, 34*(10), 2573-2585.

Haghighat Mehr, P., Voldan Zagh, M. J., Tajik, R., Jabari, S., Sahebi, M. R., Islami, R., Ganjian, M., & Dehghani, M. (2012). The analysis of the time series of Hashtgerd subsidence using radar interferometry and global positioning system, *Journal of Geosciences*, (85).

Hajizadeh A.H., Nasim Mahlah, M. A., Farzaneh S., Rastegar A. M., Seyyed Razaei, H. (2013). Principles of Microwave Remote Sensing (Radar Interferogram) with Emphasis on Earth Sciences. Satellite Publishing, Tehran.

Hoffmann, J., Zebker, H. A., Galloway, D. L., & Amelung, F. (2001). Seasonal subsidence and rebound in

Las Vegas Valley, Nevada, observed by synthetic aperture radar interferometry. *Water Resources Research, 37*(6), 1551-1566.

Poland, J. F., Ireland, R. L., Lofgren, B. E., & Pugh, R. G. (1975). Land subsidence in the San Joaquin Valley, California, as of 1972.

Li, C., Tang, X., & Ma, T. (2006). Land subsidence caused by groundwater exploitation in the Hangzhou-Jiaxing-Huzhou Plain, China. *Hydrogeology Journal, 14*(8), 1652-1665.

Motagh, M., Djamour, Y., Walter, T. R., Wetzel, H. U., Zschau, J., & Arabi, S. (2007). Land subsidence in Mashhad Valley, northeast Iran: results from InSAR, levelling and GPS. *Geophysical Journal International, 168*(2), 518-526.

Motagh, M., Walter, T. R., Sharifi, M. A., Fielding, E., Schenk, A., Anderssohn, J., & Zschau, J. (2008). Land subsidence in Iran caused by widespread water reservoir overexploitation. *Geophysical Research Letters, 35*(16).

Motagh, M., Djamour, Y., Walter, T. R., Wetzel, H. U., Zschau, J., & Arabi, S. (2007). Land subsidence in Mashhad Valley, northeast Iran: results from InSAR, levelling and GPS. *Geophysical Journal International, 168*(2), 518-526.

Motagh, M., Djamour, Y., Walter, T., Moosavi, Z., Arabi, S., & Zschau, J. (2006). Mapping the Spatial and Temporal Pattern of Landsubsidence in the City of Toos, Northeast Iran, Using Theintegration of InSAR, Continuous GPS and Precise leveling. *Geophysical Research Abstracts,. 8*, 07881.

Pacheco, J., Arzate, J., Rojas, E., Arroyo, M., Yutsis, V., & Ochoa, G. (2006). Delimitation of ground failure zones due to land subsidence using gravity data and finite element modeling in the Querétaro valley, México. *Engineering Geology, 84*(3-4), 143-160.

Mather, P. M., & Koch, M. (2011). *Computer processing of remotely-sensed images: an introduction*. John Wiley & Sons.

Pope, J. P., & Burbey, T. J. (2004). Multiple-aquifer characterization from single borehole extensometer records. *Groundwater, 42*(1), 45-58.

Richards, J. A. (2009). *Remote sensing with imaging radar* (Vol. 1). Berlin: Springer.

Hunt, R. E. (2007). *Geologic hazards: a field guide for geotechnical engineers*. CRC Press.

Schoeneberger, P.J. & Wysocki, D.A., (1997). Geological of geology , American Geological Institute,Alexandria, National Soil Survey Center, 4th Ed, p 769. ISBN 0-922152-34-9

Sharifi Kia, M. (1991). Determination of the extent and amplitude of ground submarine by radar interferometry (D-InSAR) method in Navek-Bahreman plain. *Journal of Planning and Space Design, 16*(3), 55-77.

Sharifikia, M. (2006). DEN Generation & Morphology Feature Extraction – Using InSAR, PGD Project Submitted to CSSTEAP.

Sharifikia, M. (2009). D-InSAR Data Processing and Analysis for Mapping Land Subsidence Phen omenon In Rafsanjan Area, Iran M.Tech Thesis, Submitted to Andra University-India.

Sharifikia, M., DEM Generation & Morphology Feature Extraction -Using InSAR, PGD Project Submitted to CSSTEAP, 2006.

Shemshaki, A., Blourchi, M. J., & Ansari, F. (2005). Preliminary report on Tehran subsidence. *Engineering Geology Scientific report to the Geological Survey of Iran, Tehran*.

Tony, W. G., Martin, C., & Fred, G. B. (2005). *Sinkhole and Subsidence*. Springer and Praxis Publishing Ltd. UK -Germany.

Zebker, H. A., Rosen, P. A., Goldstein, R. M., Gabriel, A., & Werner, C. L. (1994). On the derivation of coseismic displacement fields using differential radar interferometry: The Landers earthquake. *Journal of Geophysical Research: Solid Earth, 99*(B10), 19617-19634.